

State selected ion–molecule reactions by a TESICO technique. X. $O^+ 2(v)+CH_4$

Kenichiro Tanaka, Tatsuhisa Kato, and Inosuke Koyano

Citation: *The Journal of Chemical Physics* **84**, 750 (1986); doi: 10.1063/1.450572

View online: <http://dx.doi.org/10.1063/1.450572>

View Table of Contents: <http://scitation.aip.org/content/aip/journal/jcp/84/2?ver=pdfcov>

Published by the [AIP Publishing](#)

Articles you may be interested in

State selected ion–molecule reactions by the TESICO technique. XIII. Vibrational state dependence of the cross sections in the reaction $C_2D^+ 2(v_2)+H_2$

J. Chem. Phys. **86**, 688 (1987); 10.1063/1.452271

State selected ion–molecule reactions by a TESICO technique. XII. Internal energy dependence of the relative cross section and mechanism branching of the reaction $CH^+ 4(v) +CH_4 \rightarrow CH^+ 5 +CH_3$ and its isotopic variants

J. Chem. Phys. **85**, 5705 (1986); 10.1063/1.451530

State selected ion–molecule reactions by a TESICO technique. VII. Isotope effect in the reactions $O_2^+(X\ 2\Pi_g, a\ 4\Pi_u)+HD \rightarrow O_2^+ H+(O_2D^+)+D(H)$

J. Chem. Phys. **79**, 4302 (1983); 10.1063/1.446365

State selected ion–molecule reactions by a TESICO technique. VI. Vibronic state dependence of the cross sections in the reactions $O^+(X\ 2\Pi_g, v; a\ 4\Pi_u, v)+H_2 \rightarrow O_2H^++H, H^+ 2+O_2$

J. Chem. Phys. **77**, 4441 (1982); 10.1063/1.444446

State selected ion–molecule reactions by a TESICO technique. V. $N_2^+(v)+Ar \rightarrow N_2+Ar^+$

J. Chem. Phys. **77**, 834 (1982); 10.1063/1.443899



State selected ion–molecule reactions by a TESICO technique. X.

$O_2^+(v) + CH_4$

Kenichiro Tanaka, Tatsuhisa Kato,^{a)} and Inosuke Koyano
Institute for Molecular Science, Myodaiji, Okazaki 444, Japan

(Received 24 June 1985; accepted 1 October 1985)

Vibrational state selected (relative) reaction cross sections have been determined for $v = 0-3$ of the O_2^+ ion, for each of the three product channels of the reaction $O_2^+(v) + CH_4$, viz.



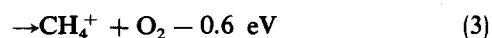
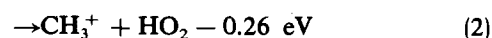
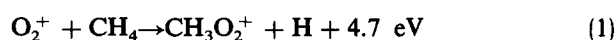
using the TESICO (threshold electron–secondary ion coincidence) technique. At a fixed collision energy of 0.27 eV, it has been found that the cross section of exoergic channel (1) increases most prominently with increasing vibrational quantum number v in the range $v = 0-2$, but decreases sharply in going from $v = 2$ to $v = 3$. The cross sections of endoergic channels (2) and (3) also increase with increasing v but their rates of increase are much smaller than that of channel (1) in the range $v = 0-2$. When v is increased to 3, however, charge transfer channel (3) is enhanced dramatically and the CH_4^+ ion becomes the most abundant product ion. The cross section of channel (2) also increases more sharply in going from $v = 2$ to $v = 3$ than in the range $v = 0-2$, but the CH_3^+ ion still remains the least abundant of the three product ions. As a result of these variations in the individual cross sections, the overall cross section for the $O_2^+ + CH_4$ reaction increases monotonically with increasing v throughout the range studied ($v = 0-3$). The results are compared with that of the collision energy dependence as obtained in drift and flow-drift experiments and the implications are discussed in conjunction with the structure of the $CH_3O_2^+$ ion and the relevant potential energy surfaces.

I. INTRODUCTION

The reaction of O_2^+ with CH_4 has long been the subject of intensive studies from the viewpoints of chemistry in the stratosphere¹⁻³ and CH_4/O_2 combustion flames.^{4,5} Recently, much interest centered on its dynamical aspects, since several experimental studies⁶⁻⁹ have revealed that its rate constant varies in an interesting manner as a function of temperature or collision energy; at room temperature, the rate constant is very small, having a value $k \sim 6 \times 10^{-12} \text{ cm}^3 \text{ s}^{-1}$.^{1,5,6} This increases up to $\sim 2 \times 10^{-10} \text{ cm}^3 \text{ s}^{-1}$ when the mean relative kinetic energy is increased to 1 eV in a flow-drift tube^{6,9} or a drift tube.⁷ The recent study on the temperature dependence of this reaction using a selected ion flow tube (SIFT) and an expanding jet apparatus has also witnessed the increase in the rate constant with increasing temperature between 300 and 560 K.⁸ However, the most remarkable finding of the latter study is the rapid increase of this rate constant with decreasing temperature below 300 K, reaching a value $k = 4.7 \times 10^{-10} \text{ cm}^3 \text{ s}^{-1}$ at 20 K, the lowest temperature studied. Furthermore, the data showed that the rate constant approaches the collisional limiting value k_c when extrapolated to absolute zero of temperature.

The extent of increase in the rate constant with increas-

ing mean relative kinetic energy in drift or flow-drift experiments depends largely on the nature of the rare gases used as a buffer.^{6,7} For example, a larger enhancement of the rate constant is observed in Ar and Kr than in He buffer gas. This fact has been interpreted as due to the internal (vibrational) excitation of the O_2^+ ions by collisions with the heavier buffer gas atoms. In fact, vibrational quenching experiments^{10,11} have shown that the vibrationally excited O_2^+ ions are deactivated by argon and not by helium, a fact from which it is inferred, based on microscopic reversibility arguments, that the O_2^+ ions in a drift tube can be vibrationally excited in argon buffer but not in helium buffer.¹² However, no direct information on the reactions of vibrationally excited O_2^+ ions with CH_4 has been reported so far. In the present paper, we report the first measurements of the vibrational state selected (relative) reaction cross sections for the three channels of the reaction of O_2^+ with CH_4 , viz.



for $v = 0-3$ of the O_2^+ ion at a fixed collision energy of $0.27 \pm 0.13 \text{ eV}$.

^{a)} Present address: Department of Chemistry, Kyoto University, Kyoto 606, Japan.

II. EXPERIMENTAL

The experimental technique used is the TESICO,¹³ which utilizes the detection of mass-analyzed reaction products (secondary ions) in coincidence with the threshold electrons ejected when reactant ions (primary ions) are produced by photoionization of parent molecules. The technique and the apparatus named TEPSICO have been described in detail.¹³ In the present study, the double chamber mode of operation,¹³ i.e., a beam-gas mode, is used and the light source is the many-line emission spectrum of hydrogen with a monochromator bandwidth of about 0.5 Å.

The threshold electron analyzer of the original apparatus is replaced in the present experiment by an indirect analyzer which utilizes non-line-of-sight trajectories of threshold electrons to the detector.¹⁴ A schematic of the analyzer of our new design is shown in Fig. 1. Subject to the field gradient produced by a voltage difference between the top electrode and the pair of the lower electrodes (see the A-A' cross section, lower drawing), the threshold electrons entering this region through the entrance hole centered at the axis (S_1), follow a trajectory direct to the exit hole (of the same diameter) located at an off-axis position (S_2). Energetic electrons entering this region follow different trajectories due to the different velocity component in the axial direction and thus get rid of detection. This arrangement is found to give 4–5 times more intense threshold electron signals than our original analyzer system,¹³ which is a combination of a line-of-sight steradiancy analyzer and a hemispherical electrostatic analyzer. This improvement in the threshold electron intensity enabled the use of the double chamber mode of operation for the present reactions which have very small cross sections.

III. RESULTS AND DISCUSSION

A. Threshold electron spectrum of O_2

A portion of the threshold electron spectrum of O_2 relevant to the present study is shown in Fig. 2. The region corresponding to the higher vibrational states of the O_2^+

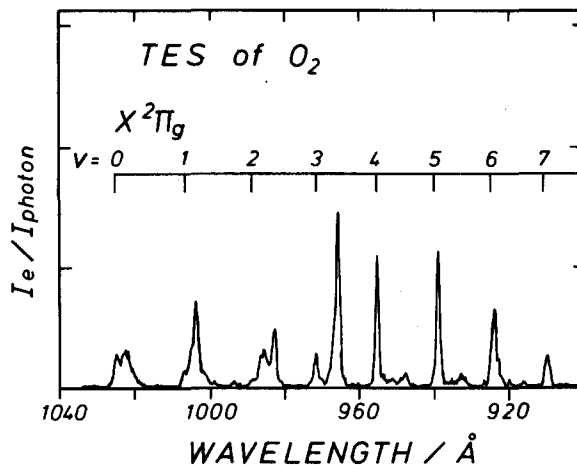


FIG. 2. Threshold electron spectrum of O_2 in the region corresponding to lower vibrational states of the O_2^+ ($X^2\Pi_g$) ion. Threshold positions indicated by vertical bars with ν number are taken from spectroscopic data. (Ref. 16).

ground $X^2\Pi_g$ state and vibrational states of the excited $a^4\Pi_u$, $A^2\Pi_u$, and $b^4\Sigma_g^-$ states has been presented elsewhere.¹⁵

In Fig. 2, it is seen that most of the strong peaks do not occur at the exact threshold wavelengths for the ionic vibrational states¹⁶ (indicated by vertical lines) but rather occur at somewhat shorter wavelengths than the exact values. These peaks evidently originate from autoionization processes producing near-threshold electrons, i.e., those autoionizing to the closest-lying ionic vibrational state. These near-threshold electrons are transmitted through the analyzer due to its finite resolution width, although the transmission efficiency is much lower than that for the true threshold electrons. The fact that these near-threshold electrons constitute strongest peaks despite their low transmission efficiency indicates that ions in this wavelength region are overwhelmingly produced through autoionization and not by direct ionization. This near-degenerate autoionization is conveniently utilized in the present study as an effi-

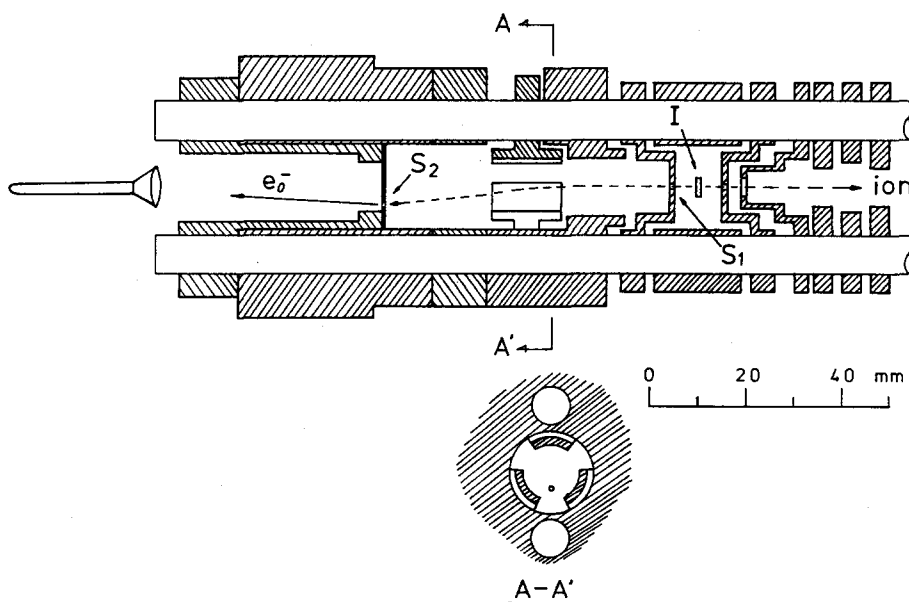


FIG. 1. Non-line-of-sight steradiancy analyzer for threshold electrons. I: ionization region; S_1 , S_2 : entrance and exit hole, respectively, of the steradiancy analyzer.

cient way to produce ions in some vibrational states of interest.

Threshold electron spectrum of O_2 has previously been studied by three research groups.¹⁷⁻¹⁹ Guyon and Nenner¹⁷ used synchrotron radiation with 0.5 Å bandwidth and time-of-flight electron energy analysis with 20 meV electron energy resolution. Stockbauer¹⁸ used hydrogen many-line spectrum/helium Hopfield continuum with 1.2 Å bandwidth and a 127° cylindrical plate analyzer. Chutjian and Ajero,¹⁹ on the other hand, utilized their TPSA detection to obtain threshold electron spectra. While gross features of the spectra obtained by these authors and ourselves resemble one another, there exist some discrepancies among them concerning some detailed aspects such as relative intensities of particular two peaks. These discrepancies undoubtedly result from differences in photon bandwidth, electron energy resolution, and the nature of the light source used. In the following state selected measurements of ion-molecule reactions, use was made of the wavelengths that give the highest threshold electron intensity in a narrow range below the threshold for each vibrational state of interest. These chosen wavelengths do not necessarily coincide with a strongest peak in Fig. 2, the latter showing threshold electron intensity divided by photon intensity.

B. State selected cross sections of reactions (1)–(3)

Relative reaction cross sections for the individual vibrational states v ($v = 0-3$) of the O_2^+ (${}^2\Pi_g$) reactant ion have been determined at a fixed center-of-mass collision energy of 0.27 ± 0.13 eV for each of reaction channels (1)–(3). These are determined, as described in previous papers,¹³ directly from the ratio of the integrated intensities of the time-of-flight coincidence peaks for the primary and secondary ions. Experimental results are summarized in Fig. 3. Error bars indicate uncertainties of the determination, mainly coming from statistical errors.

Several interesting features are immediately evident from Fig. 3. Cross section for channel (1) is found to increase sharply as the vibrational quantum number v increases from 0 to 2, although the reaction is highly exoergic even with $v = 0$. The cross section then decreases sharply in going from $v = 2$ to $v = 3$, the $v = 3$ value being almost the same as that for $v = 1$. Endoergic channels (2) and (3), which have negligibly small cross sections when $v = 0$, become significant at $v = 1$ and are further enhanced at $v = 2$, although their cross sections still remain much smaller than that for channel (1). When the vibrational quantum number is further increased to $v = 3$, however, the increase in the cross section for channel (3) is dramatic and the CH_4^+ ion becomes by far the most abundant product ion. Channel (2) is also enhanced considerably at $v = 3$, the cross section being of almost the same magnitude as that for channel (1).

We have previously studied²⁰ the same reactions using the single chamber mode of operation¹³ up to $v = 2$. Although collision energy distribution in that mode is rather broad and only the average collision energy \bar{E}_{cm} is defined, the essential feature of the results obtained at $\bar{E}_{cm} = 0.2$ eV agrees with that of the $v = 0-2$ portion of the present result.

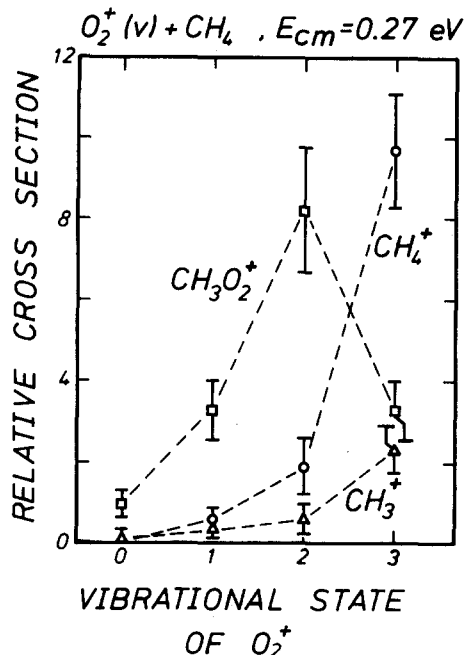
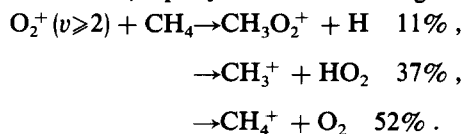


FIG. 3. State selected cross sections for reactions (1)–(3). States selected are vibrational states ($v = 0-3$) of the O_2^+ (${}^2\Pi_g$) ion. Center-of-mass collision energy is indicated.

Possible enhancement of the overall reaction rate for the $O_2^+ + CH_4$ reaction by vibrational excitation of O_2^+ has previously been suggested by Dotan *et al.*⁶ and Alge *et al.*⁷ in a flow-drift tube and a drift tube experiment, respectively. Both of these groups found that the extent to which the rate coefficient is increased as the mean relative kinetic energy is increased above ~ 0.06 eV is much larger for argon buffer gas than for helium buffer gas used in these experiments. They suggested, as a possible interpretation, that the difference could have arisen from drift-induced internal (vibrational) excitation of the O_2^+ ions in the heavier argon buffer gas, premising that the vibrationally excited ions have higher reactivity toward methane. Recently, Durup-Ferguson *et al.*⁹ studied the reaction and quenching of the vibrationally excited O_2^+ ions with CH_4 , using a monitor ion technique to probe the vibrational state distribution of the O_2^+ ions in a flow-drift tube. They showed that, at thermal energies, $O_2^+(v = 1)$ is rapidly quenched by CH_4 , while $O_2^+(v \geq 2)$ reacts with CH_4 rapidly with the following branching ratio:



From this branching ratio and the vibrational state distribution, as well as the fact that only $O_2^+(v \geq 3)$ can undergo charge transfer reaction at thermal energies, they further proceeded to conclude that $O_2^+(v \geq 3)$ react exclusively by channel (3) and $O_2^+(v = 2)$ reacts by channels (1) and (2) with a branching ratio of about 1:3.

The present results show, in a direct manner, that the vibrational excitation of the O_2^+ ions up to $v = 3$ indeed enhances the overall reactivity of these ions with methane. In addition, our results clearly indicate that this enhancement for $v = 1$ and 2 is primarily due to the enhancement of the

exoergic channel producing $CH_3O_2^+$, and not due to the existence of endoergic channels that become accessible for these excited states as was assumed in the previous studies.^{6,7} The enhanced overall reaction rate for the $v = 3$ ions is indeed seen to be due to the opening of the endoergic channels, especially the charge transfer channel producing CH_4^+ . However, considering the relative populations of the $v = 1$ – 3 ions in the drift or flow-drift tubes under usual conditions, it would obviously be incorrect to assume that the enhancement of the reactivity by possible vibrational excitation in drift experiments is due to the accessibility of the endoergic channels. For instance, at the vibrational temperature of ~ 3000 K (assuming that an “equilibrium” temperature is reached), the population ratios $v = 1 : v = 2 : v = 3$ of the O_2^+ ions are calculated to be 1 : 0.41 : 0.017, using the vibrational constants for O_2^+ ($X^2\Pi_g$), $\omega_e = 1904.8$ cm^{-1} and $\omega_e\chi_e = 16.26$ cm^{-1} .²¹ From these ratios and our data on the relative cross sections (Fig. 3), we calculate the contributions of the three individual reaction channels (1)–(3) to the vibrationally enhanced portion of the overall reaction as 74%, 8%, and 18%, respectively. Thus the contribution of the endoergic channels is only 26%.

In reaction dynamics, it is of importance to inquire whether different forms of reactant energy are equally effective in promoting endoergic reactions or in enhancing (or suppressing) exoergic reactions, or some reactions have inclination to a certain form of reactant energy. In order to see this point, we compare in Fig. 4 our overall reaction rates with those from the flow-drift experiment,^{6,9} as a function of total reactant energy ($E_{trans} + E_{vib}$). Our relative cross section for $v = 0$ is normalized to the rate constant value of the flow-drift study at the same \bar{E}_{cm} .

In drift experiments, it has been customary to assume that helium buffer gas does not excite vibrational motion of drifting molecular ions even at high E/N (E is the electric field strength and N the buffer gas number density). Thus, \bar{E}_{cm} determined by the E/N value has been considered to be equal to total energy and the dependence of rate constants on \bar{E}_{cm} has been believed to represent the pure kinetic energy effect without suffering any influence of the internal excitation. If this is true, the good agreement (within experimental error) of the total energy dependence of the overall reaction rate between our (circles) and the flow-drift (solid line curve) results would indicate that the vibrational energy of the reactant ion and the relative translational energy are equally effective in enhancing this reaction.

Very recently, however, it has been shown by Federer *et al.*²² that considerable vibrational excitation of molecular ions occurs in drift tubes even with helium buffer gas. In the case of O_2^+ drifting in helium, their result shows that a vibrational temperature (T_v) of about 2000 K is reached at an E/N value of ~ 80 Td, meaning that up to $\sim 20\%$ of the ions are vibrationally excited. Thus, the solid curve in Fig. 4 must be considered to include the influence of both relative kinetic and vibrational energies, while the variation of our data represents pure vibrational energy effect. Therefore, the pure kinetic energy effect of these \bar{E}_{cm} regions must be considerably smaller than that shown by the solid line curve. The comparison in Fig. 4, combined with the above considera-

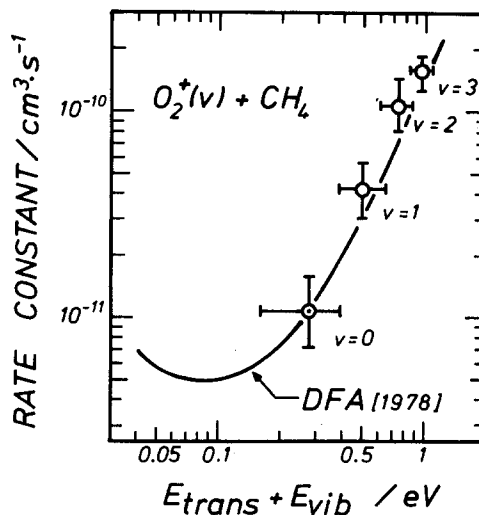


FIG. 4. Rate constant for the overall reaction of O_2^+ with CH_4 , as a function of total energy ($E_{trans} + E_{vib}$). Open circle: present result; solid line curve (DFA): results from flow-drift experiment (Ref. 6). Our data are normalized to the flow-drift data at $v = 0$.

tion, thus indicates, at least qualitatively, that vibrational energies are more effective than collision energies in enhancing the reaction of O_2^+ with CH_4 in these collision energy regions.

The relative translational energy dependence of the rate constants for individual channels (1)–(3) has also been reported recently in a flow-drift experiment.⁹ Here, use was made of He buffer gas with sufficient amount of added O_2 , and thus the O_2^+ reactant ions are claimed to be completely in $v = 0$. Their result shows that the most abundant ion at 1 eV (the highest energy studied) is CH_3^+ , in contrast to our result for $v = 3$ (total energy $E_{trans} + E_{vib} = 0.95$ eV) which shows that by far the most abundant ion is CH_4^+ . The relative abundance of the $CH_3O_2^+$ ion is also different between the two experiments. These apparent discrepancies in the product distribution may also indicate the different roles of vibrational and translational energies in promoting these reactions.

There has been considerable controversy concerning the structure of the $CH_3O_2^+$ ion. Lindinger and co-workers first reported that the $CH_3O_2^+$ product of reaction (1) has the structure of protonated formic acid, $HC(OH)_2^+$, based on two different kinds of experiments. In the first experiment,²³ in which the isotopic exchange reaction of the $CH_3O_2^+$ product of reaction (1) with D_2O was compared with the same reaction of the $CH_3O_2^+$ ion produced by the reaction of formic acid with its own molecular ion, they found that successive exchange of two H atoms occurs for the $CH_3O_2^+$ ions from both sources but no exchange of the third H atom occurs even at highly elevated D_2O densities, suggesting the existence of two OH hydrogen atoms and one CH hydrogen atom in both ions. In the second experiment,²⁴ where collision induced breakup with Ar was compared between the $CH_3O_2^+$ ions from the above two sources, they again obtained the identical results for the ions from both sources; the breakup gave equal amounts of H_3O^+ and HCO^+ at all col-

lision energies above threshold. From these comparisons, they reached the above conclusion.

However, this conclusion was recently denied by Ferguson and co-workers²⁵ based on studies of a large number of reactions which the product $CH_3O_2^+$ ion of reaction (1) undergoes but protonated formic acid does not. From these reaction studies, they concluded that the $CH_3O_2^+$ product of reaction (1) is methylene hydroperoxy cation H_2COOH^+ .

In any case, reaction (1) turns out to be an intriguing elementary reaction, since the formation of the $CH_3O_2^+$ ion from O_2^+ and CH_4 requires considerable rearrangement of the constituent atoms. Moreover, the reaction has recently been studied at very low temperatures down to 20 K using a new expanding jet and a selected ion flow tube, with rather remarkable results⁸: The small room temperature rate constant increases markedly as the temperature is lowered, reaching half the collisional rate constant k_c at 20 K. When the temperature dependence $k = CT^{-1.8}$ obtained in the low temperature region is extrapolated to the absolute zero, the rate constant exactly reaches k_c , the collisional limiting value. In order to interpret these experimental results, Rowe *et al.*⁸ proposed a detailed reaction mechanism, which also reasonably interprets the above mentioned drastic rearrangements involved in the reaction.

According to that model, hydride ion (H^-) transfer from CH_4 to O_2^+ first takes place in the $O_2^+ \cdot CH_4$ electrostatic potential well upon initial encounter of the reactants. Although the formation of free CH_3^+ and HO_2 [channel (2)] is endoergic by 0.26 eV, the endoergicity is easily supplied by the electrostatic attraction energy between them, due to the large dipole moment (2.1 D²⁶) of HO_2 . At thermal energies and lower, the products are thus trapped in their electrostatic potential well upon formation at a close encounter distance. This trapped product pair $(CH_3^+ \cdot HO_2)^*$ is the intermediate complex from which unimolecular decomposition may take place either to the reactants or to the exoergic products $CH_3O_2^+ + H$.

The supposition of the $(CH_3^+ \cdot HO_2)$ complex is supported by the fact that it greatly assists the rearrangements required for reaction (1). Namely, one of the C-H bonds is broken and the O-H bond is formed already in the complex. All these facts suggest that the complex $(CH_3^+ \cdot HO_2)^*$ is dyn-

amically on the way to the products $CH_3O_2^+ + H$. Obviously, it is also on the way to the products $CH_3 + HO_2^+$, which indeed are observed above threshold.

The decomposition of the complex to the $CH_3O_2^+$ product still requires rearrangement. This presumably is some concerted motion of constituent atoms, with which potential energy barrier is expected to be associated. Also, there should be a barrier between the colliding $CH_4O_2^+$ state and the H^- transfer products $CH_3^+ \cdot HO_2$. Thus the system may represent a case in which at least two potential barriers are involved along the reaction coordinate, as schematically shown in Fig. 5.

Then the vibrational energy effect as observed in the present study, as well as the collision energy and temperature effect observed in other experiments, should reflect the dynamics of the system around these two barriers. The first barrier A (Fig. 5) seems to be easily overpassed or circumvented in both directions, considering the high efficiency of the reaction at extremely low temperatures and of the back decomposition of the complex at higher temperatures. That means, the complex is better considered as $[O_2^+ \cdot CH_4]^* \leftrightarrow [CH_3^+ \cdot HO_2]^*$. Then the observed characteristics of the reaction must be related to the second barrier B. Several possible cases may be speculated concerning the dynamical situation around this barrier. For example, a possibility would be the case in which the second potential barrier B is actually quite low but the path on the potential energy surface leading to the product is so narrow (because of the concerted nature of the process) that the system cannot easily find the way. Thus at room temperatures or higher, the complex overwhelmingly decomposes back to the reactants, giving very small rate constants for forward reaction. As the temperature is lowered, the lifetime of the complex (with respect to the back decomposition) becomes longer and longer and the probability that the complex eventually find the way to the product is increased accordingly. Vibrational excitation of the reactant ion might then enhance the reaction probability by allowing the system to reach the product without taking this narrow path.

It is also possible to consider cases in which the second barrier is very high, being close to the level of the reactants, or even higher than that level and the reaction proceeds via

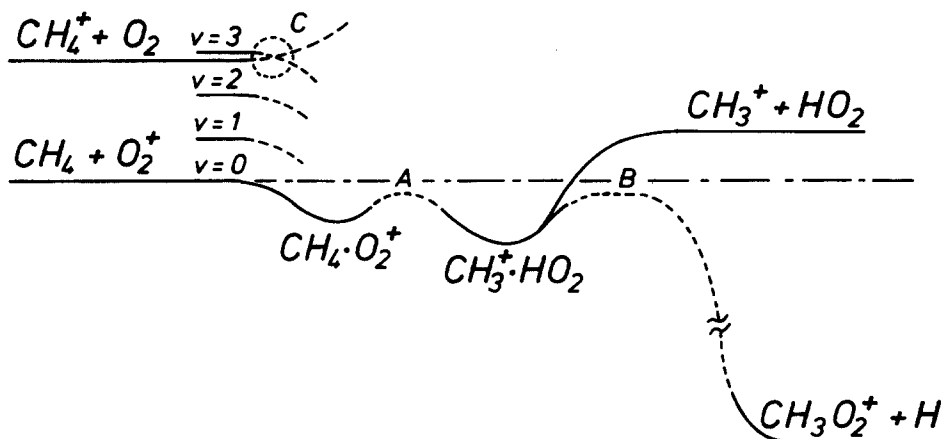


FIG. 5. A schematic diagram showing potential energy variation along reaction coordinates.

tunneling. In any case, however, the situation around here must be much more complicated than is conceived from the conceptual drawing in Fig. 5, since many low lying excited electronic states are expected for the $CH_3^+ \cdot HO_2$ complex. Evidently, further experimental and theoretical work is needed to clarify the dynamics of this reaction.

The charge transfer products $CH_4^+ + O_2$ obviously correlates to a different (excited) potential energy surface from that correlating to the reactants, and the reaction involves nonadiabatic transitions between them. This transition would take place at an early stage of reactants' encounter (C in Fig. 5), perhaps at intermolecular distances even larger than the Langevin radius. Our present results indicate that the probability of the transition is greatly enhanced when the reactant ion is excited to $v = 3$. This large enhancement would certainly be due to the exoergic nature of the reaction for $v = 3$, but might also result from the fact that the reactant and product states are in close energy resonance ($\Delta E = -0.03$ eV). In this context it would be of interest to examine the reactions of $v = 4$. Unfortunately, however, this has been impossible owing to the very weak threshold electron intensity at the threshold wavelength for $v = 4$.

The vibrational energy of $O_2^+ (v = 2)$ combined with the *cm* collision energy of 0.27 eV is also sufficient to overcome the endoergic nature of the charge transfer channel. The experimental result indeed shows a significant rise in the $v = 2$ cross section but also may indicate that this combined amount of energy is not so efficient in promoting the reaction as pure vibrational energy that exceeds the endoergic nature. The sharp decrease in the $CH_3O_2^+$ cross section at $v = 3$ (Fig. 3) is evidently caused by the competition with this charge transfer channel at the early stage of the encounter, and thus may not carry much information about the dynamics in the complex region.

IV. CONCLUSION

We have determined the relative reaction cross sections for each of the three channels of the $O_2^+ + CH_4$ reaction [reactions (1)–(3)] as a function of the vibrational quantum number v of the reactant ion ($v = 0-3$). At a fixed collision energy of 0.27 eV, it has been found that the predominant consequence of the vibrational excitation is the enhancement of the exoergic rearrangement channel [reaction (1)] for $v = 1$ and 2, while it is the dramatic enhancement of the endoergic charge transfer channel [reaction (3)] for $v = 3$. The latter channel, once it becomes exoergic, competes with rearrangement channels, thus reducing the sum of the cross sections for reactions (1) and (2) at $v = 3$.

The reaction system $O_2^+ + CH_4$ is of great interest since it involves three distinct types of reactive channels; electron transfer, H^- transfer, and deep rearrangement process. The effect of vibrational excitation on the rates of these individual channels as observed here should certainly bear information about the potential energy surfaces and the dynamics involved. Several possible cases have been speculated which may explain both the present results and the results on the temperature and collision energy dependence. Clearly further work is necessary, both experimentally and theoretically, to identify which dynamics is actually operative.

¹V. Nestler and P. Warnek, *Chem. Phys. Lett.* **45**, 96 (1977).

²D. Smith, N. G. Adams, and T. M. Miller, *J. Chem. Phys.* **69**, 308 (1978).

³I. Dotan, J. A. Davidson, F. C. Fehsenfeld, and D. L. Albritton, *J. Geophys. Res.* **83**, 4036 (1978).

⁴J. L. Franklin and M. S. B. Munson, Tenth International Symposium on Combustion, Pittsburgh, 1965, pp. 561–568.

⁵B. R. Hollebone and D. K. Bohme, *J. Chem. Soc. Faraday Trans. 2* **69**, 1569 (1973).

⁶I. Dotan, F. C. Fehsenfeld, and D. L. Albritton, *J. Chem. Phys.* **68**, 5665 (1978).

⁷E. Alge, H. Villinger, and W. Lindinger, *Plasma Chem. Plasma Proc.* **1**, 65 (1981).

⁸B. R. Rowe, G. Dupeyrat, J. B. Marquette, D. Smith, N. D. Adams, and E. E. Ferguson, *J. Chem. Phys.* **80**, 241 (1984).

⁹M. Durup-Ferguson, H. Böhringer, D. W. Fahey, F. C. Fehsenfeld, and E. E. Ferguson, *J. Chem. Phys.* **81**, 2657 (1984).

¹⁰H. Böhringer, M. Durup-Ferguson, D. W. Fahey, F. C. Fehsenfeld, and E. E. Ferguson, *J. Chem. Phys.* **79**, 4201 (1983).

¹¹H. Böhringer, M. Durup-Ferguson, E. E. Ferguson, and D. W. Fahey, *Planet. Space Sci.* **31**, 483 (1983).

¹²Very recently, it has been shown that the O_2^+ ions are also vibrationally excited even in He buffer gas. See discussion below and Ref. 22.

¹³I. Koyano and K. Tanaka, *J. Chem. Phys.* **72**, 4858 (1980).

¹⁴W. B. Peatman, G. B. Kasting, and D. J. Wilson, *J. Electron Spectrosc.* **7**, 233 (1975).

¹⁵K. Tanaka, T. Kato, P. M. Guyon, and I. Koyano, *J. Chem. Phys.* **77**, 4441 (1982).

¹⁶P. H. Krupenie, *J. Phys. Chem. Ref. Data* **1**, 423 (1972).

¹⁷P. M. Guyon and I. Nenner, *Appl. Opt.* **19**, 4068 (1980).

¹⁸R. Stockbauer, *Adv. Mass Spectrom.* **8**, 79 (1980).

¹⁹A. Chutjian and J. M. Ajello, *Chem. Phys. Lett.* **72**, 504 (1980).

²⁰K. Tanaka, T. Kato, and I. Koyano, *At. Collision Res. Jpn.* **9**, 73 (1983); *Annu. Rev. Inst. Mol. Sci. Jpn.* **1983**, 97.

²¹K. P. Huber and G. Herzberg, *Molecular Spectra and Molecular Structure. IV. Constants of Diatomic Molecules* (Van Nostrand Reinhold, New York, 1979).

²²W. Federer, H. Ramler, H. Villinger, and W. Lindinger, *Phys. Rev. Lett.* **54**, 540 (1985).

²³H. Villinger, R. Richter, and W. Lindinger, *Int. J. Mass Spectrom. Ion Phys.* **51**, 25 (1983).

²⁴H. Villinger, A. Saxer, R. Richter, and W. Lindinger, *Chem. Phys. Lett.* **96**, 513 (1983).

²⁵E. E. Ferguson (private communication).

²⁶S. Saito and C. Matsumura, *J. Mol. Spectrosc.* **80**, 34 (1980).